J. Fluid Mech. (1975), *vol.* 71, *part* 2, *pp.* 385–405
Printed in Great Britain

The deepening of a mixed layer in a stratified fluid

By P. F. LINDEN

Department of Applied Mathematics and Theoretical Physics,
University of Cambridge

(Received 10 September 1974)

In this paper two aspects of the deepening of a mixed layer in a stratified fluid are examined in the laboratory. The first is the deepening of a layer into a region of constant density gradient. Turbulence is produced by an oscillating grid which generates a horizontally homogeneous field of motion with no significant mean flow. It is found that the rate at which the potential energy of the basic stratification is increased by the mixing does not bear a simple relationship to the rate of energy input by the grid. On the other hand, when allowance is made for the decay of turbulent energy away from the grid and only that portion to reach the bottom of the mixed layer is considered, the rate of potential energy increase is found to be proportional to this available energy. The second aspect to be discussed is the effect of energy radiation by internal waves in the region below the mixed layer. Estimates are made of the possible loss of energy to these waves, which reduces the amount available to deepen the layer. An experimental demonstration of up to 50 % reduction in the mixing rate due to the presence of internal waves is given. Finally, the implications of these results are discussed in the light of current theoretical models of the deepening process.

1. Introduction

The amount the oceanic thermocline deepens during the passage of a storm or owing to convective motions induced by cooling at the ocean surface is an important aspect of the general question of the interaction of the atmosphere and ocean. This phenomenon has many features in common with the equivalent process of the rising of the atmospheric inversion during the course of the day due to wind mixing and convective heating. Both of these phenomena have been the subject of considerable interest over the past few years but, although the basic physical processes have been identified, understanding of the details of the deepening is in many cases superficial. The current state of knowledge of the subject is summarized by two recent papers. Niiler (1975) gives a comprehensive description of the energetics of the deepening of the upper mixed layer of the ocean and shows that the energy and momentum input at the surface is proportioned into mean and turbulent energy of the layer. Both of these types of motion are then available to mix fluid across the thermocline thereby increasing the potential energy of the water column. A model of the deepening of the atmospheric boundary layer has been presented by Carson (1973).

It is not the object of this paper to discuss the details of attempts to model

these phenomena. Indeed the atmospheric case will not explicitly be discussed further although much of what will be said will be relevant to that case also. The aim of this paper is to isolate in the laboratory two aspects of the deepening process, and to relate the consequences of the experiments in terms of these models. Within the assumption that the deepening of the wind-mixed upper layer can be considered as a one-dimensional process, we isolate in the first instance the effect on the deepening rate of the decay of turbulent energy as the depth of the thermocline increases. This is done by generating a horizontally homogeneous field of turbulent motion at the top of a water column which has a linear increase in density with depth. The turbulent motions are generated in such a way that there is no significant mean flow; consequently the relative importance of the mean flow and the turbulent motions in deepening the layer can be assessed by comparison with other experiments where this feature is included (e.g. Kato & Phillips 1969). A comparison is made between the rate of change of the potential energy of the water column due to mixing and the rate of input of kinetic energy at the surface. It is shown that these do not bear a simple relationship to one another, although in theoretical models it is usually assumed that they are proportional (Niiler 1975).

The second feature which is isolated in these experiments is the effect of removal of energy from the turbulent motions by internal wave radiation. When the region below the thermocline is stably stratified the action of the turbulent motions on the thermocline can excite internal waves in this region. These waves may then propagate energy away to great depths thereby leaving less energy available for the deepening of the layer. This feature too has been ignored in the theoretical models to date. By carefully controlling the geometry and density stratification a significant reduction in the mixing rate has been observed when a density gradient has been present in the region below the turbulent layer.

The paper is divided up in the following way. In § 2 the experiments are described and the various means of monitoring the deepening of the mixed layer are discussed. In § 3 the penetration of the mixed layer into a constant density gradient is discussed. Some theoretical ideas are investigated and then compared with the experimental results. In § 4 the effect of internal waves is examined, by first discussing the parameter range over which they are important and then giving an experimental example of the reduction in mixing rate. The details of the internal wave motions generated by the turbulent motions are examined. The implications of these results with regard to theories of the deepening of the thermocline are discussed in § 5.

2. The experiments

The experiments were carried out in a rectangular Perspex tank 25·4 × 25·4 cm in cross-section and 46 cm deep. Turbulence was generated by oscillating a horizontal grid consisting of 1 cm square bars in a 5 × 5 array with 5 cm between the centres. The grid was oscillated vertically with a stroke of 1 cm, with frequencies up to 5 Hz. This grid and tank have been used for mixing experiments on several occasions (Turner 1968; Crapper & Linden 1974); details of the turbulence

generated by this apparatus in a homogeneous fluid have been measured and related to the frequency and amplitude of the grid oscillation by Thompson & Turner (1975). They found that the r.m.s. horizontal velocity u' of the turbulence decays with increasing distance z from the grid and is given by

$$u' = 1{\cdot}4\omega z^{-\frac{3}{2}} z_0^{\frac{5}{2}} \text{ cm/s},$$

where ω is measured in hertz, and the integral length scale of the turbulence l is related to the distance from the grid by

$$l = 0{\cdot}1z \text{ cm}.$$

Here z_0 is the stroke length of the grid oscillations (1 cm).

The penetration of a turbulent layer into a region of density variation was studied by filling the tank with a stable salt stratification. Three types of stratification were used in order to isolate different aspects of the deepening process. In every case the grid was positioned at a mean depth of 6 cm below the free surface, which was 40 cm above the bottom. The region above the grid was always kept homogeneous by the turbulence and initially contained fresh water. In the first series of experiments, designed to study the penetration into a constant density gradient, the region below the grid was filled with a salt solution such that the density increased linearly with distance from the grid. The experiment was started by turning on the motor which vibrated the grid; the depth and characteristics of the mixed layer were then monitored at discrete times thereafter.

In the second series of experiments a different initial stratification was used. It was intended to isolate the effects of internal wave radiation on the mixing process at a density interface. This was achieved by setting up a two-layer initial stratification with the interface at a distance of 7 cm below the grid. The stirring was then begun and the rate of descent of the interface measured. The experiment was then repeated with the lower homogeneous layer replaced with one in which the density increased linearly with depth and the rates of descent compared. In order to ensure that the only significant difference between the two runs was the presence or absence of a gradient beneath the interface it was necessary to ensure that the interface only deepened a small amount. In this context 'small' is defined in relation to the length $\Delta\rho/\rho_z$, where $\Delta\rho$ is the density difference across the interface and ρ_z the gradient in the layer below. By suitably adjusting the parameters it was found that the density step across the interface at the conclusion of the measuring period could be kept within 3 % of the initial value of $\Delta\rho$. Further evidence that the situation was properly controlled was provided by the observed fact that the rate of descent of the interface was constant over the measurement period (see figure 5).

The characteristics of the mixed layer and the stratified layer were determined using a conductivity probe (see Crapper & Linden (1974) for details of the measurement system). Profiles of conductivity *vs.* depth were obtained by rapidly traversing the probe vertically downwards (at a fixed horizontal position) at various times during an experiment, thereby obtaining an effectively instantaneous profile, which was converted to density units by calibration. The probe was also used to obtain some indication of the wave motions generated at and

below the interface by the turbulence. This was done by measuring the conductivity at a point as a function of time. This proved to be reasonably satisfactory at or quite near the interface. However, at moderate distances below the interface the extremely slow motion of fluid past the probe tip did not appear to be sufficient to wash away the polarization field which builds up there. Consequently, spurious and quite unrealistic readings were obtained under these conditions.

The depth of the mixed layer was usually determined visually from a shadowgraph. As a result of fluctuations of the interface the depth of the mixed layer was uncertain by $\pm 0{\cdot}1$ cm in some cases. The results of these measurements were confirmed by the conductivity–depth profiles. A further method of visualization was to place neutrally buoyant beads in the tank; with these it was also possible to obtain an estimate of the wave motions generated by the turbulence.

Details of the wave motions propagating in the gradient region beneath the interface were obtained by suspending aluminium particles in the water and then slit lighting the tank from the side. The wave motions were observed to be very slow so time-lapse movies were made which, when projected at normal speeds giving a 10–20 fold increase in speeds, showed quite clearly the wave motions generated. These movies were then analysed to give some indication of the phase speeds, group velocity and wavenumber of the waves.

3. Increase in depth of the mixed layer and the formation of the thermocline

Theoretical considerations

Consider the turbulent energy equation for a mixed layer with no mean shear, which takes the form (Niiler 1975)

$$\frac{1}{2}\frac{\partial}{\partial t}\overline{q'^2}+\frac{\partial}{\partial z}\left[\overline{w'\left(\frac{p'}{\rho_0}+\frac{q'^2}{2}\right)}\right]=-\frac{g}{\rho_0}\overline{w'\rho'}-\nu\overline{\nabla\mathbf{u}'.\nabla\mathbf{u}'}, \tag{1}$$

where the turbulent velocity field $\mathbf{u}'=(u',v',w')$, $q'^2=u'^2+v'^2+w'^2$, p' is the perturbation pressure, ρ' the density perturbation, ρ_0 the mean density, g the acceleration due to gravity and ν the kinematic viscosity. In the absence of a buoyancy input both terms on the right-hand side of (1) are negative and they represent the extraction of energy from the turbulence by a turbulent buoyancy flux and viscous dissipation ϵ. Integrating (1) across the mixed layer from the grid to the interface we have

$$\left[\overline{w'\left(\frac{p'}{\rho_0}+\frac{q'^2}{2}\right)}\right]_{\text{int}}=\left[\overline{w'\left(\frac{p'}{\rho_0}+\frac{q'^2}{2}\right)}\right]_{\text{grid}}-\frac{g}{\rho_0}\int\overline{w'\rho'}\,dz-\int\epsilon\,dz, \tag{2}$$

provided the turbulent kinetic energy is independent of time (as is the case in our experiments). Equation (2) states that the turbulent energy at the interface is the value input at the grid minus that removed by the buoyancy flux and dissipation in the layer.

In his model Niiler (1975) calculates the rate at which the layer would deepen by assuming that the energy required to accelerate the fluid entrained is equal to the energy available at the interface as represented by the term on the left-

hand side of (2). In order to relate the rate of deepening to the input at the surface (the energy source for the oceanic case and equivalent to the grid in these experiments), it is necessary to estimate the remaining dissipative terms on the right-hand side of (2). Niiler (1975), in keeping with previous authors, makes the simplest possible assumption, namely that the energy available at the interface is a constant fraction of the surface input independent of the depth of the mixed layer. There appears to be no *a priori* justification for this assumption and it is made purely for convenience. We shall now investigate the consequences of this assumption in the context of our experiments.

Consider a stratified water column where the density $\rho(z)$ is given by

$$\rho = \begin{cases} \bar{\rho}, & -d < z < 0, \\ \rho_0 - \Gamma(z+D_0), & -H < z < -d, \end{cases} \tag{3}$$

where the z axis is taken as positive upwards. Here d represents the depth of the mixed layer and H the total depth of the fluid column. Then under the condition that the total mass in a vertical column is conserved, i.e.

$$\int_{-H}^{0} \rho \, dz = \text{constant},$$

the potential energy of the column is given by

$$V = \int_{-H}^{0} g\rho z \, dz = \tfrac{1}{12} g\Gamma d^3 - \tfrac{1}{4} g\Gamma D_0^2 d + \tfrac{1}{2} g\Delta\rho_0 D_0 d + \text{constant},$$

where $\Delta\rho_0 = \rho_0 - \bar{\rho}$, when $d = D_0$, is the initial density step.

Hence

$$dV/dt = \tfrac{1}{4}\rho_0 N^2 (d^2 - D_0^2)\dot{d} + \tfrac{1}{2} g\Delta\rho_0 D_0 \dot{d}, \tag{4}$$

where N is the buoyancy frequency of the column below the mixed layer, given by

$$N^2 = -\frac{g}{\rho_0}\frac{d\rho}{dz} = \frac{g\Gamma}{\rho_0}.$$

In the experiments to be described in this section there is no initial density step, i.e. $\Delta\rho_0 = 0$, and so the second term on the right-hand side of (4) is zero.

The rate of input of kinetic energy by the grid is proportional to $\rho_0\omega^3$, where ω is the frequency of oscillation (the amplitude remaining fixed). The assumption that the rate of change of the potential energy of the water column is proportional to the rate of energy input by the grid implies that

$$D(D + 2D_0)\, dD/dt = c_1 \omega^3 / N^2. \tag{5}$$

Here $d = D + D_0$, where D_0 is the depth of water above the grid (kept constant at 6 cm in our experiments) and D is the depth of the mixed layer measured from the grid. c_1 is an unknown constant of proportionality. With the initial condition that $D = 0$ when $t = 0$ we find

$$D^2(D + 3D_0) = 3c_1 \omega^3 N^{-2} t. \tag{6}$$

If the numerical value of D_0 is substituted into (6) it may then be solved explicitly. However, for our present purposes it is sufficient to note two limits.

During the initial stages when $D \ll D_0$, $D \propto t^{\frac{1}{2}}$, whilst in the later stages of the experiment when $D \gg D_0$, $D \propto t^{\frac{1}{3}}$.

In the case of the present experiments, though, it is possible to estimate the amount of kinetic energy in the turbulent motions at the interface directly. As was mentioned in § 2, Thompson & Turner (1975) have measured the r.m.s. horizontal velocity u' of the turbulent motions as a function of the distance from the grid. Hence we can now make a comparison equivalent to (6) but where the rate of production of kinetic energy at the interface is included explicitly. The rate at which kinetic energy arrives at the interface is given by $\frac{1}{2}\rho_0\overline{(2u'^2+w'^2)w'}$; assuming that $w' \sim u'$ we estimate this as $\frac{3}{2}\rho_0 u'^3$, where $u' = u'(z)$ as given by Thompson & Turner (1975) (see § 2). If it is now supposed that the potential energy changes at a rate proportional to the rate of input of kinetic energy at the interface we have

$$D^{\frac{11}{2}}(D+2D_0)\,dD/dt = 6(1{\cdot}4)^3 c_2 \omega^3 N^{-2} z_0^{\frac{15}{2}}, \tag{7}$$

where z_0 is the stroke length of the grid oscillations (1 cm). c_2 is a dimensionless constant whose value indicates the fraction of kinetic energy converted to potential energy. Solving (7) we find (with $z_0 = 1$ and $D_0 = 6$)

$$D^{\frac{13}{2}}(\tfrac{1}{15}D+\tfrac{12}{13}) = 3(1{\cdot}4)^3 c_2 \omega^3 N^{-2} t. \tag{8}$$

Taking the limits of short and long times as before we have

$$D \propto \begin{cases} t^{\frac{2}{13}}, & z_0 \ll D \ll D_0, \\ t^{\frac{2}{15}}, & D \gg D_0. \end{cases}$$

These results show a much reduced rate of growth of the mixed layer compared with that obtained when it is assumed that a constant fraction of the grid input is available to increase the potential energy of the system.

The experimental results

When the stirring was initiated the turbulence penetrated to some finite depth almost immediately (usually $\sim$ 2–3 cm in the first minute). After this initial stage a turbulent mixed layer formed which then penetrated gradually into the region of constant density gradient. Figure 1 shows a series of three density–depth profiles taken at approximately 10 min intervals which exhibits this deepening of the mixed layer. The main features to notice on these profiles are that the upper layer is uniform and then the density gradient increases to a maximum in the 'thermocline' which has been formed by erosion of the density gradient. Beneath the thermocline the density gradient decreases to the value in the fluid beneath. This lower gradient remains the same throughout the experiment. Figure 2 shows a plot of the buoyancy frequency against depth. The value of the density gradient was obtained by averaging successive sets of 10 data points and then differencing these averages; as approximately 250 data points were collected for each profile this method gives 24 readings of the gradient spaced vertically at about 0·4 cm. Figure 2 shows that a significant density interface has been established at the bottom of the mixed layer with a thickness of about 1·5 cm.

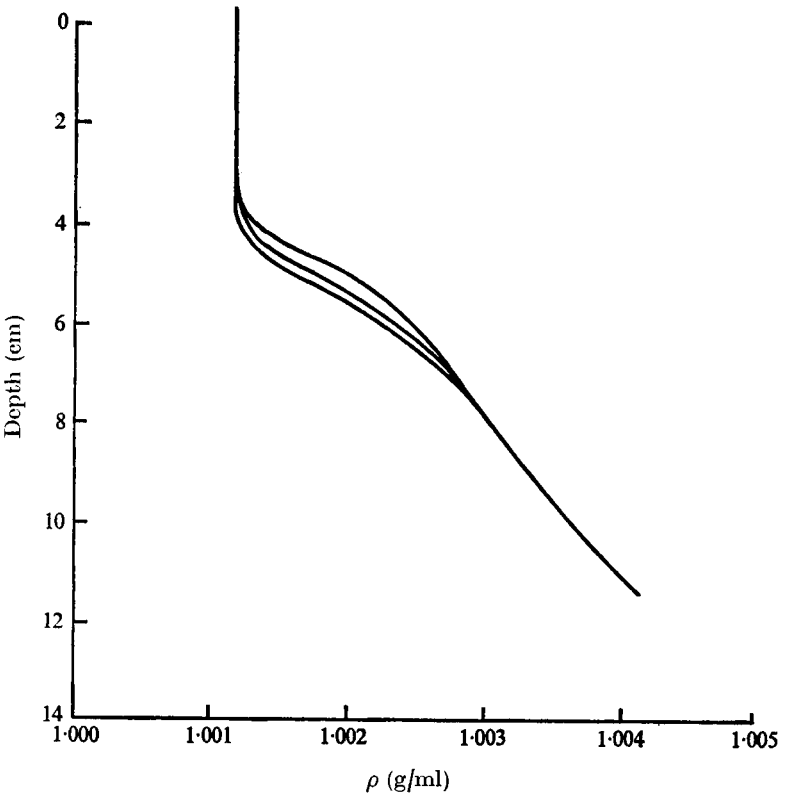

FIGURE 1. The penetration of a mixed layer into a constant density gradient, as shown by three density–depth profiles taken approximately 10 min apart. Note that as the deepening progresses the upper layer remains well mixed and that the density gradient is unchanged; the build-up of a 'thermocline' at the bottom of the mixed layer is observed. These profiles are reproduced (smoothed) from the output of the conductivity probe; the depth scale has an arbitrary origin.

The density profiles shown on figure 1 are very similar in appearance to those obtained in the upper regions of the ocean. Kitaigorodskii & Miropol'skii (1970) have analysed several density profiles obtained at ocean weather ships at various times of the year and found that they can be non-dimensionalized in order to give a 'universal profile'. The non-dimensionalization is achieved by defining

$$T = [\rho_u - \rho(z,t)]/[\rho_u - \rho_h], \quad \zeta = [z - D(t)]/[h - D(t)],$$

where ρ_u is the density of the upper mixed layer of depth $D(t)$ and h is a reference depth (where the density is ρ_h) below which the stratification remains constant in time. They hypothesize that $T \equiv T(\zeta)$ and plot the oceanic data accordingly. We gave done an equivalent plot for the density profiles taken in these experiments. Figure 3 shows a typical plot of $T(\zeta)$ against ζ, the values of $\zeta < 0$ corresponding to values in the mixed layer. The profile so obtained shows good qualitative agreement with those given by Kitaigorodskii & Miropol'skii (1970).

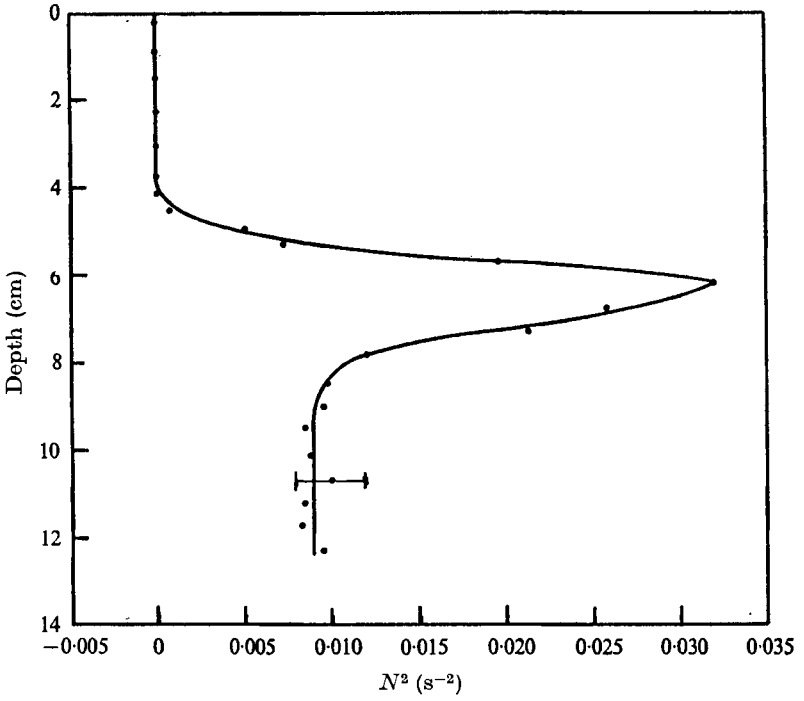

FIGURE 2. A plot of the square N^2 ($= -g\rho_0^{-1}\, d\rho/dz$) of the buoyancy frequency obtained by differencing averages of successive sets of data points from a profile similar to that shown on figure 1. The intensification of the gradient at the bottom of the mixed layer is reflected in the peak in the N^2 *vs.* depth curve. The depth scale has an arbitrary origin.

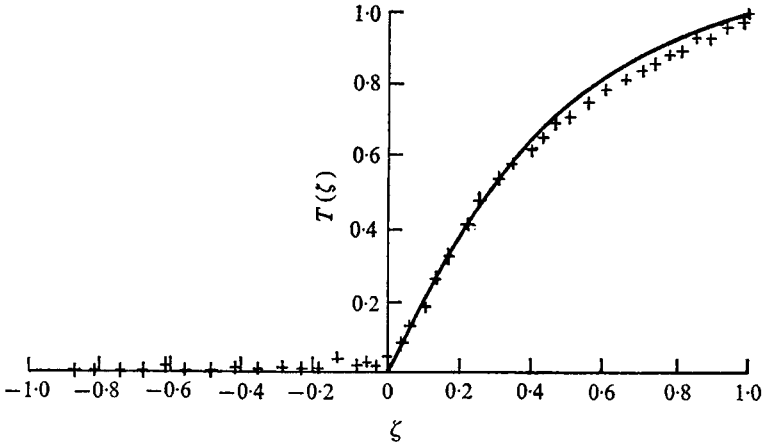

FIGURE 3. The dimensionless density profile obtained from a density–depth profile such as that shown in figure 1. T is a dimensionless density co-ordinate and ζ a dimensionless depth co-ordinate. $\zeta \leqslant 0$ corresponds to the mixed layer and $0 \leqslant \zeta \leqslant 1$ to the region through the interface to a reference depth in the stable layer. For this case the stratification in the stable layer has buoyancy frequency $N^2 = 0{\cdot}01\ \mathrm{s}^{-2}$. ——, $T(\zeta) = 2\zeta - \frac{6}{5}\zeta^2 + \frac{1}{5}\zeta^4$; see § 3.

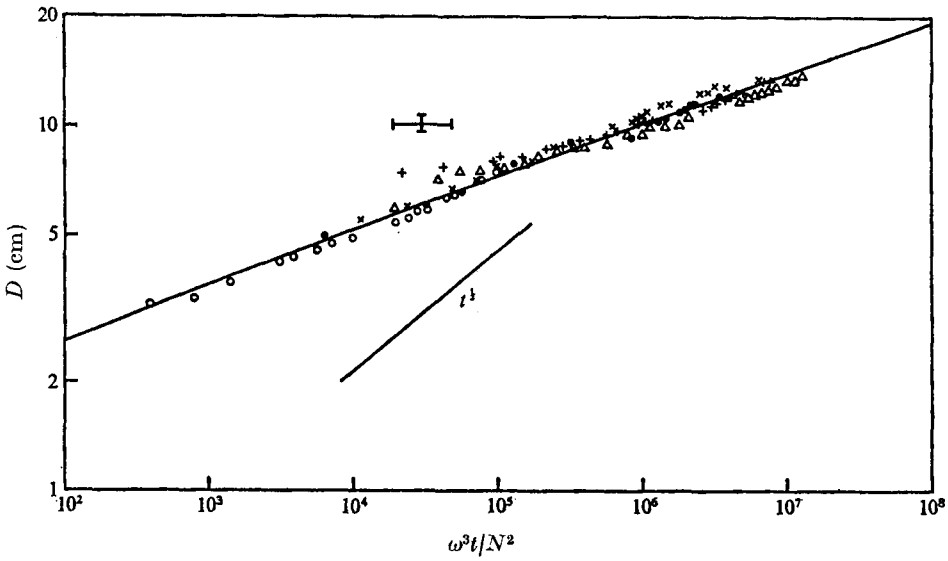

FIGURE 4. A plot of the depth of the mixed layer below the grid D as it penetrates a constant density gradient against the time t after the stirring was begun non-dimensionalized with respect to the grid frequency ω and the buoyancy frequency N. The experimental points represent five separate runs: ●, $N^2 = 0{\cdot}009\ \mathrm{s}^{-2}$, $\omega = 3{\cdot}3$ Hz; ×, $N^2 = 0{\cdot}015\ \mathrm{s}^{-2}$, $\omega = 5$ Hz; ○, $N^2 = 0{\cdot}017\ \mathrm{s}^{-2}$, $\omega = 1{\cdot}7$ Hz; △, $N^2 = 0{\cdot}005\ \mathrm{s}^{-2}$, $\omega = 5$ Hz; +, $N^2 = 0{\cdot}009\ \mathrm{s}^{-2}$, $\omega = 5$ Hz. The error bars represent the maximum possible uncertainty in the experimental points. ——, equation (8) with the coefficient c_2 adjusted to give a best fit to the data.

It is possible to obtain an approximate analytic expression for $T(\zeta)$ for $0 \leqslant \zeta \leqslant 1$. For the experimental run shown on figure 3 this is

$$T(\zeta) = 2\zeta - \tfrac{6}{5}\zeta^2 + \tfrac{1}{5}\zeta^4$$

(see the appendix), which is plotted as the full curve on figure 3. The agreement with our data is quite satisfactory.

The depth of the mixed layer as a function of time is plotted (logarithmically) on figure 4. Five runs were carried out with different N and ω, and the time scale is non-dimensionalized with respect to the parameter ω^3/N^2. The solution to (8) is plotted for comparison with the value of c_2 adjusted to give the fit shown. This fit is for $c_2 = 0{\cdot}61$. Also shown is a line proportional to $t^{\frac{1}{3}}$, which is the slowest rate of deepening given by a solution to (6). The implications of this figure are first that the non-dimensional grouping $\omega^3 t/N^2$ provides a good collapse of the data (the wayward points are generally those found at the beginning of a run before the system has settled down). This means that relating the change in potential energy of the basic stratification to the input of kinetic energy into the system in the simple manner assumed above is satisfactory. Second, the fact that (8) describes the deepening rate very accurately whilst (6) overestimates it implies that it is necessary to consider only the energy available at the interface in the above energy balance, and that this will not remain a constant fraction of the energy input at the grid as the layer deepens.

The value of c_2 required to give the fit to the data should not be given undue emphasis. The main reason for the uncertainty in the value of c_2 derives from assuming $w' \sim u'$ in the expression for the turbulent kinetic energy. The fact that the results scale with this assumption is some *a posteriori* justification for its use. However, if w' differs from u' by a factor of two, say, then the kinetic energy supply rate will differ by a factor of four. With this kind of uncertainty and the uncertainty in the measurement of u' itself (Thompson & Turner 1975) the possible uncertainty in c_2 is such that it may be in error by a factor of eight. However this implies that $0{\cdot}1 \leqslant c_2 \leqslant 1$.

At this point it is useful to relate these results to those obtained in similar experiments, notably those of Turner (1968). Turner found that it was possible to relate the non-dimensional entrainment rate $E = \dot{d}/u'$ across a density interface between two homogeneous layers to a local interfacial Richardson number Ri_I defined in terms of the density step across the interface and the turbulent velocity and length scales near the interface. The energy argument presented above is approximately equivalent to assuming a relationship between E and Ri_I of the form $E \propto Ri_I^{-1}$. However, Turner (1968) found that for a salt interface $E \propto Ri_I^{-\frac{3}{2}}$. In order to resolve this difference an attempt was made to reformulate the results shown on figure 4 by determining E as a function of Ri_I as each run progressed. It proved to be very difficult to do this with any degree of confidence, the errors involved in differentiating the depth *vs.* time curve and evaluating Ri_I at each depth being very large. Consequently, it was not possible to determine the dependence of E on Ri_I, if, indeed, such a unique dependence exists. When the results were examined in this way, a range of power laws was obtained, with exponents varying from approximately $-1{\cdot}5$ to $-0{\cdot}7$. The value of the exponent depended on the gradient in the deep layer and the distance of the interface from the grid. This indicates that the deepening rate can not be determined uniquely by a local interfacial parameter when a density gradient exists on one side of the interface. One additional feature which has so far been excluded is the effect of internal waves generated in the deep layer and this will be discussed in the following section. In fact, although the overall behaviour of the data shown on figure 4 is described satisfactorily by (8), closer examination reveals that individual runs show some deviation from the curve described by this equation. This point will be taken up in more detail in § 5.

4. Internal waves in the stable layer beneath the interface

Theoretical considerations

The effect of the radiation of energy and momentum away from the mixed layer by internal waves propagating in the region below the thermocline has largely been ignored by earlier investigators of the problem of the deepening of the upper mixed layer. Townsend (1966) has examined the effect of the impact of turbulent motions on a region of fluid containing a stable density gradient. He showed that, in principle, the internal waves generated can radiate away a significant amount of energy but so far no explicit demonstration of this has been given. In the present context it is conceivable that sufficient energy may be removed by

the internal waves and that the energy available for changing the potential energy of the fluid column by mixing across the interface will be significantly reduced.

In order to investigate the conditions under which such a reduction in energy is likely to occur we note the following. If internal waves of amplitude a and wavelength λ are generated in a region with buoyancy frequency N then (Thorpe 1973) the maximum possible vertical energy flux per unit horizontal area carried by the waves is given by

$$F = \rho_0 a^2 N^3 \lambda / 3\pi\sqrt{3}. \tag{9}$$

It is appropriate to compare this energy flux with the observed rate of change of potential energy of a fluid column of unit horizontal area, given in § 3 as

$$F_1 = \tfrac{1}{4}\rho_0 N^2 \dot{d}(d^2 - D_0^2) + \tfrac{1}{2} g \Delta\rho_0 D_0 \dot{d},$$

where d is the depth of the mixed layer. Initially $d = D_0$ and the density step at $z = -D_0$ is $\Delta\rho_0$. The ratio A of these two energy fluxes gives an indication of the importance of the internal wave radiation:

$$A = \frac{4}{3\pi\sqrt{3}} \frac{a^2 \lambda N}{[(d^2 - D_0^2) + 2RD_0^2]\dot{d}}, \tag{10}$$

where $R = g\Delta\rho_0/\rho_0 N^2 D_0$. When $N = 0$, no internal waves can exist beneath the interface and $A = 0$, indicating that no energy is lost; as A increases the internal waves remove relatively more energy from the region of the interface.

The experimental results

Measurements of the mixing rate. Several runs were made which demonstrate the reduction of the mixing rate due to the presence of a density gradient in the fluid below the interface. The results of two of these runs are shown on figures 5(*a*) and (*b*). In each case the figure shows plots of the increase in depth of the mixed layer as a function of time. Two runs are shown on each figure; one consists of the deepening of a layer when there is no gradient beneath the interface, and the second shows the increase in depth for an interface with the same initial step but now with a gradient in the lower layer. Both sets of data show that the deepening rate is reduced by the presence of a gradient in the lower layer, and in each case the reduction is consistent with the value of A determined from (10). (The details of how A was estimated are given below.) At a given depth the rate of potential energy increase of the water column is proportional to the rate of descent of the interface. Consequently a 10 % reduction in the rate of descent of the interface is consistent with $A \approx 0{\cdot}1$, indicating a loss of about 10 % of the energy to internal waves (see figure 5*a*). Similarly, on figure 5(*b*), $A \approx 1$ implies that about half of the energy is lost by internal wave radiation, and this is consistent with the observed 50 % reduction in the rate of descent of the interface.

The reduction in the entrainment rate as a function of the buoyancy frequency N of the stratification beneath the interface is shown on figure 6. The data shown on this figure were obtained by comparing the entrainment rates for varying N whilst holding the density step $\Delta\rho_0$, the turbulent intensity u' and the position

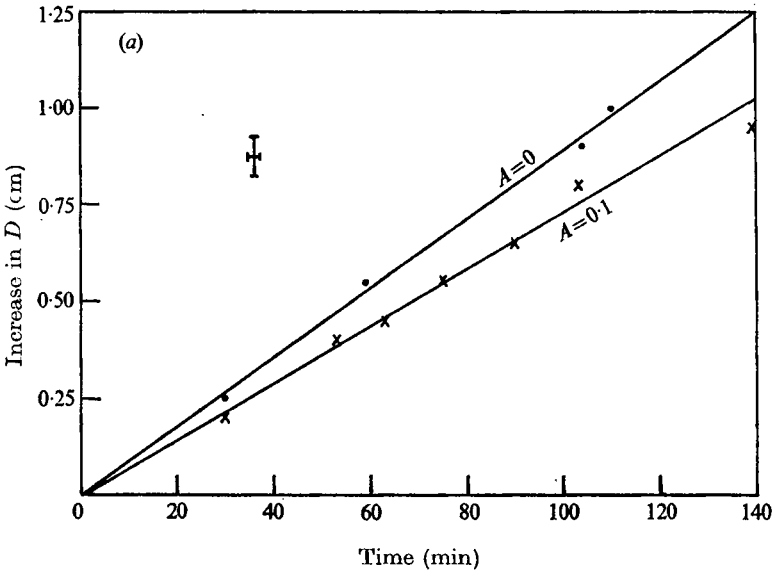

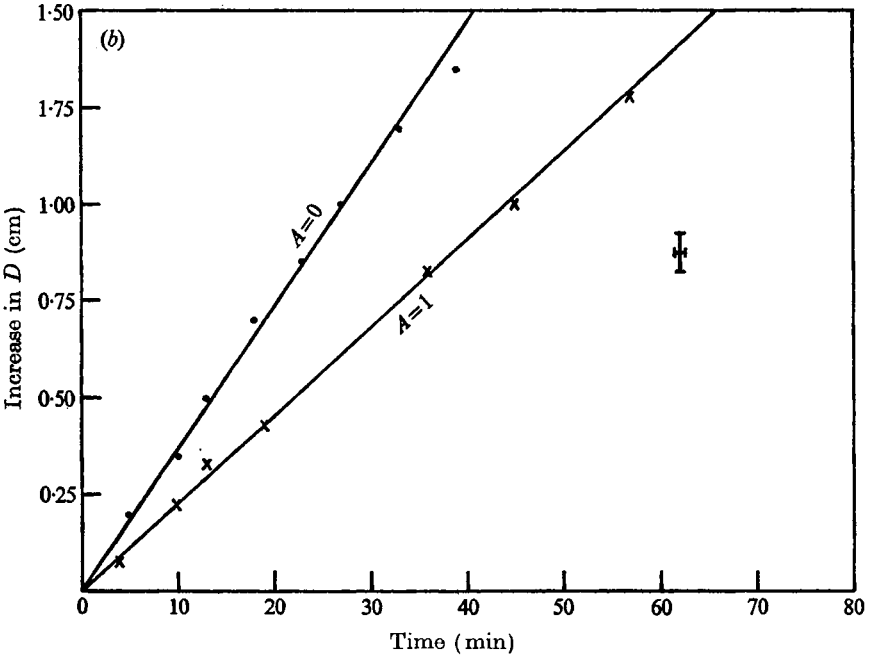

FIGURE 5. The increase in depth of the mixed layer D (in all cases the mixed layer was 13 cm deep initially with the grid 6 cm below the free surface) as a function of the time after the stirring was begun. The grid frequency ω was 5 Hz. The parameter A denotes the expected fraction of energy lost to internal waves radiated in the lower layer (see § 4 for a definition). The error bars represent the maximum uncertainty in the experimental points. The straight lines are best fits to the data; the slope of these lines is a measure of the rate at which fluid is entrained across the interface. (*a*) Initial density step $\Delta\rho_0 = 0{\cdot}030$ g/ml; ●, uniform lower layer, $N_2 = 0$; ×, linear density stratification in lower layer, $N^2 = 0{\cdot}035\,\mathrm{s}^{-2}$. (*b*) $\Delta\rho_0 = 0{\cdot}010$ g/ml; ●, $N^2 = 0$; ×, $N^2 = 0{\cdot}059\,\mathrm{s}^{-2}$.

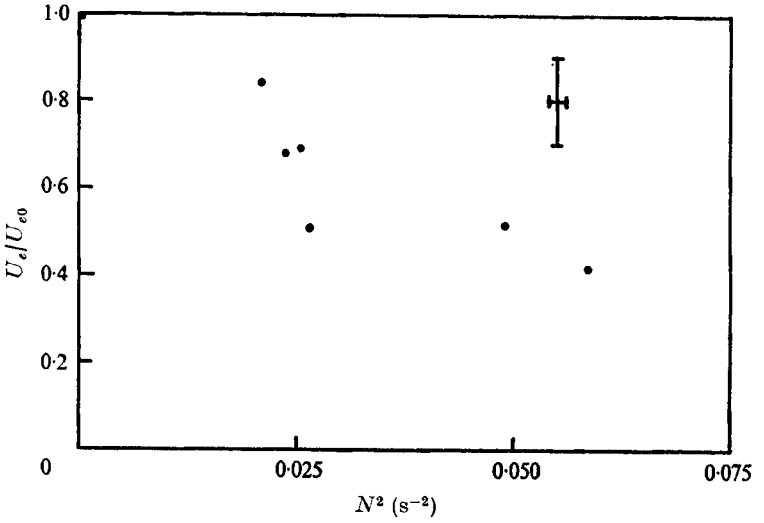

FIGURE 6. The rate of descent U_e of the interface, normalized with respect to the value U_{e0} obtained when the lower layer is homogeneous, plotted against the square N^2 of the buoyancy frequency of the lower layer. The values are appropriate to an interface with an interfacial Richardson number of 104. The error bars give estimates of the maximum errors in the data.

of the interface relative to the grid constant. This figure shows the value of the rate of descent of the interface normalized with respect to the value when $N = 0$. It is seen that the entrainment across the interface decreases as N increases, consistent with the notion that the reduction is due to the loss of energy by internal wave radiation.

The internal wave motions in the stable layer. So far we have only discussed the internal waves indirectly, through their ability to reduce the rate of deepening of the mixed layer. It is instructive now to look in some detail at the wave motions themselves and to see how they are related to the imposed forcing by the turbulence in the mixed layer. Time-lapse movies of aluminium particles suspended in the flow were made and from these it was possible to obtain a visualization of the wave motions in a plane parallel to the front wall of the tank (which we shall denote as the x, z plane).

The most striking feature of the wave motions revealed by the movies was the presence of phase lines moving upwards from the bottom of the tank to the interface. As the vertical component of the group velocity of internal waves is in the opposite direction to the vertical component of the phase velocity this implies that energy, being transmitted at the group velocity, was being removed from the vicinity of the interface and radiated towards the bottom of the tank by the waves. By measuring the orientation, spacing and speed of these phase lines it is possible to obtain information concerning the wavenumber $\mathbf{k} = (k, m)$ in the x, z plane, the frequency σ and the phase and group velocity of the waves. In fact, knowledge of the buoyancy frequency N implies that one of the observed quantities is redundant and this was used as a check on the consistency of the measurements. One movie similar to the situation shown in figure 5 (*b*) was analysed in

	θ (deg)	σ (s^{-1})	k (cm^{-1})	m (cm^{-1})
Minimum	0	0	0	1·5
Maximum	35	0·1	1·0	1·8

TABLE 1. Details of the internal wave field observed in the x, z plane in a stable layer of depth = 30 cm with buoyancy frequency $N = 0{\cdot}16\,s^{-1}$ bounded above by an interface with density step $\Delta\rho_0/\rho_0 = 0{\cdot}014$. Turbulent motions were produced by a grid approximately 5 cm above the interface oscillating with an amplitude of 1 cm and frequency of 4·6 Hz. The interfacial Richardson number based on the density step $\Delta\rho_0/\rho_0$, the r.m.s. horizontal velocity u' and the integral length scale l of the turbulence in the vicinity of the interface is approximately 100. In the above table θ is the angle between the phase lines and the horizontal, σ the frequency and k and m the wavenumbers in the x and z directions, respectively.

detail ($\Delta\rho_0/\rho_0 = 0{\cdot}014$, $Ri_I = 100, N = 0{\cdot}16\,s^{-1}$). It was found that the orientation of the phase lines varied between 0 and 35° from the horizontal. This implies a range of frequencies and wavenumbers and these are given in table 1.

It is of interest to see how these internal waves are generated. If we assume that the stratified layer reacts passively to the forcing of the interface then we must look for sources of energy in the frequency range 0–$0{\cdot}1\,s^{-1}$ in the response of the interface to the turbulent motions. Consequently, a conductivity probe was placed in the fluid and the response of the probe at fixed positions was measured as a function of time. It was found that the magnitude of the oscillations recorded in this way varied as the measuring point moved from the mixed layer into the stratified region, the amplitude increasing as the centre of the interface was approached (see figure 2) and then decreasing as the probe was lowered into the stratified layer. (As was mentioned earlier (§ 2) it was not possible to use the probe to measure the internal wave motions directly as the particle motions were very slow.) Figure 7 shows a typical conductivity trace recorded near the centre of the interface and its associated spectrum. This trace consists of 1024 data points measured at intervals of 0·1 s. The intermittent nature of the oscillations is typical and was observed at similar interfaces separating two turbulent layers (Crapper & Linden 1974). The spectrum shows the power of the signal (in arbitrary units) multiplied by the frequency plotted against the logarithm of the frequency. Plotted in this way the area under the curve in a given frequency band is proportional to the energy in that band. The spectrum shown on figure 7 shows that almost all of the energy is in the frequency range 0–$0{\cdot}5\,s^{-1}$, but with a significant amount of energy with frequencies greater than the maximum internal wave frequency observed ($0{\cdot}1\,s^{-1}$). Although it was impossible to determine the distribution of energy in the internal wave field an impression was obtained that the major contribution occurred at the higher wave frequencies observed, as the dominant pattern appeared to be phase lines propagating at an angle of 35° to the horizontal. Furthermore, the forcing at frequencies greater than $N = 0{\cdot}16\,s^{-1}$ (see figure 7) cannot produce wave motions.

A further feature of the wave field which was determined from the movie was the vertical amplitude ξ of the particle oscillations as a function of the distance D

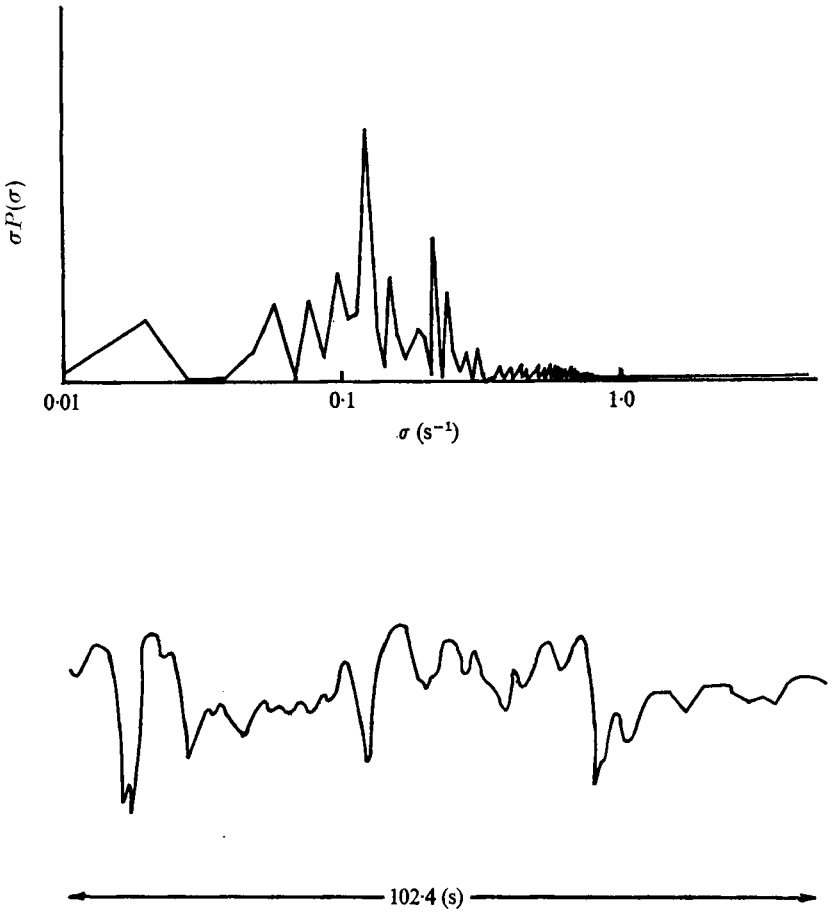

FIGURE 7. The output from the conductivity probe, converted to density units by calibration, measured at a fixed point near the centre of an interface and the corresponding spectrum. The record consists of 1024 samplings of the probe made at 0·1 s intervals. The spectrum shows the power $P(\sigma)$ of the signal multiplied by the frequency (in arbitrary units) plotted against the log of the frequency σ. For this interface $\Delta\rho/\rho_0 = 0{\cdot}010$ and the interfacial Richardson number is 115.

from the interface. Townsend (1966) has shown that beyond a critical distance D_c from the interface viscous dissipation causes decay of the internal wave amplitude. This critical distance D_c depends on the length and time scales of the impact of the turbulent motions at the top of the stable layer and on its buoyancy frequency N. Using estimates of the time scale taken from records such as those shown on figure 7 and the integral scale (§ 2) of the turbulence as the length scale we find that for the run which was analysed $D_c \approx 1$ cm. This is in agreement with the data obtained from the conductivity probe, which showed a sharp decrease in the amplitude of the fluctuations at depths greater than approximately 1 cm from the centre of the interface. The data obtained from analysis of the movie are shown on figure 8, which is a log–log plot of the normalized vertical displacement ξ/ξ_0 of the particles against the distance from the interface. Townsend (1966) showed

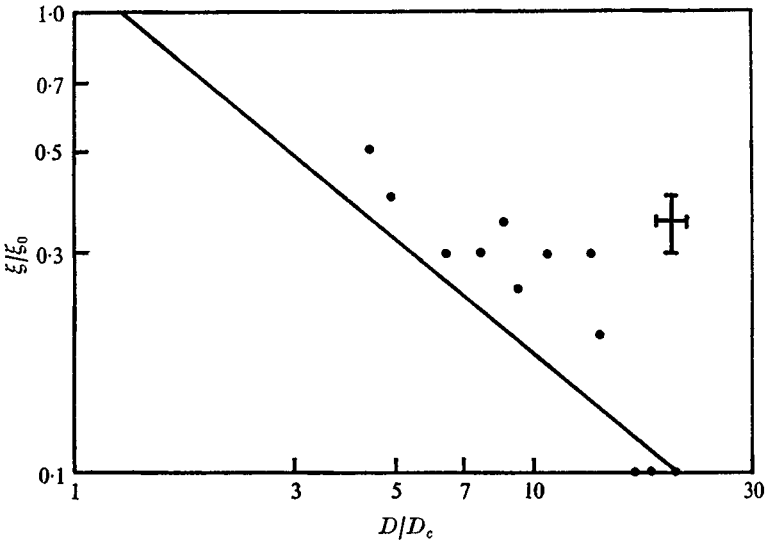

FIGURE 8. The vertical particle displacements ξ measured in the stable layer as a function of the non-dimensional distance D/D_c from the interface. The values are normalized with respect to ξ_0, the value of the particle displacements at the interface. The details of the stratification and the forcing are the same as those given in table 1. The solid line has a slope of $-\frac{5}{6}$.

that for internal waves generated by turbulent motions at the top of a layer containing a constant density gradient

$$(\overline{\xi^2}/\xi_0^2)^{\frac{1}{2}} \propto (D/D_c)^{-\frac{5}{6}},$$

where ξ_0 is the vertical displacement at the top of the stratified layer ($\xi_0 \sim 1$ cm in this experiment). A line with a slope of $-\frac{5}{6}$ is drawn on figure 8 and the data appear to conform to this power law reasonably well.

Finally, we return to the evaluation of the parameter A defined by (10). From this formula we see that we need to determine the wavelength λ and the amplitude a in order to estimate A. As viscosity causes decay of the internal waves with depth and we are seeking an upper bound on the value of A, ξ_0 (≈ 1 cm) was used as an estimate for a. The wavelength λ was estimated directly from the film and a value of 3·5 cm was taken as typical. Using these values and the appropriate values of N, $\Delta\rho_0$ and $\dot{d}$ it was then possible to determine the values of A for runs such as those shown on figure 5.

5. Discussion

There are two main conclusions to be drawn from the experiments described above. First, the rate of increase of potential energy of a water column produced by the penetration of a turbulent layer into a region of constant density gradient is proportional to the rate of input of kinetic energy by the turbulent motions at the bottom of the mixed layer. It is not, in general, proportional to the rate of

supply of turbulent energy at the top of the mixed layer. Second, under certain circumstances radiation of energy by internal waves in the region below the mixed layer will reduce the rate of deepening of the turbulent layer.

It is valuable to compare our experimental results with those of other similar experiments. Thorpe (1966) carried out an experiment to determine the rate of deepening of a turbulent layer into a region of constant density gradient. The turbulence was generated by a grid in the same manner as in our experiments but the geometry of the tank and grid were different from the present case. He found that the layer deepened with time t such that $D \propto t^p$, where $p = 0{\cdot}18 \pm 0{\cdot}02$, which is in good agreement with the results of the present experiments. The close agreement between the present results and those of Thorpe (1966) gives some credence to the notion that the results are independent of the details of the turbulence generator, and that the rates of deepening measured in these experiments are representative of situations when no mean shear flow exists in the tank. The value of the exponent p depends essentially on the rate at which the magnitude of the turbulent velocity fluctuations decays with distance from the grid. Thompson & Turner (1975) found that for all the types of grid they investigated the dependence of the turbulent velocity on the distance from the grid could be described by a power law (see § 2). This power law was also used by Bouvard & Dumas (1967) to describe the turbulent velocity generated by an oscillating plate containing an array of holes. This kind of spatial decay rate of the turbulence appears to be a fundamental feature of these types of experiments and, as Thompson & Turner (1975) showed, is a result of inertial decay and a linear change in the length scale of the turbulence with distance from the source.

In the ocean, however, the energy input by the wind is partitioned between turbulent kinetic energy and the mean flow. This situation has been modelled in the laboratory by Kato & Phillips (1969), who applied a stress at the surface of a stratified layer in an annular tank. Both a mean flow and turbulence were generated by the stress, and the interface descended at a rate proportional to $t^{\frac{1}{2}}$. It was also found that the rate at which the potential energy of the fluid increased was proportional to the rate of dissipation of kinetic energy per unit area in the turbulent layer. In his theoretical study Niiler (1975) predicts an initial rate of deepening proportional to $t^{\frac{1}{3}}$ when a constant fraction of the surface input of energy is available for mixing across the interface.

The present experiments show, however, that when there is no mean shear a much reduced rate of deepening is produced. Consequently, it appears that the presence of a mean shear allows a larger, and indeed constant, fraction of the surface energy to be transmitted to the interface. In fact, Niiler (1975) shows that for a mixed layer 100 m deep a vertical shear of order $10^{-3}\,\mathrm{s}^{-1}$ is sufficient to make the term $\overline{u'w'}\,\partial \mathrm{U}/\partial z$ significant in the equation for the perturbation kinetic energy. This production of turbulent energy at the interface by the action of the Reynolds stress on the mean shear must, therefore, be important in the experiments of Kato & Phillips (1969).

The presence of a stable stratification in the ocean beneath the thermocline is significant in that internal waves may be generated by the response of the thermocline to the motions in the wind-mixed layer. In order to estimate the

effect of this wave generation on the rate of deepening of the oceanic thermocline it is necessary to determine the value of the parameter A, which, in turn, requires a knowledge of the forcing applied by the turbulence to the thermocline. Consequently, it is necessary to know which are the most energetic scales of the motion at the bottom of the mixed layer and how these are related to the atmospheric forcing, in order to relate the internal wave generation to its energy source. An alternative description of the parameter A can be given as follows. Suppose that the wavelength λ of the internal waves is set by the scale of the forcing by the turbulent motions: then λ can be regarded as related to some integral scale of the turbulence in the mixed layer. The results of § 3 show that

$$[(d^2 - D_0^2) + 2RD_0^2]\dot{d} \propto u'^3/N^2$$

and so we can write A in the form

$$A \propto \frac{a^2}{\lambda^2}\left(\frac{N\lambda}{u'}\right)^3.$$

Linden (1973) has shown that the distortion of an interface by a vortex ring depends upon the Richardson number Ri_I (based on the density step and the size and velocity of the ring) of the impact. Therefore, applying his results directly [his equation (4.1)] to this case we find that

$$A \propto Ri_G^{\frac{3}{2}}/Ri_I^2,$$

where Ri_I is the Richardson number of the interface and $Ri_G = (N\lambda/u')^2$ is a Richardson number of the gradient region below the interface. This description shows more clearly how the importance of the internal waves depends on the relative magnitudes of the density step and the gradient in the layer beneath. When the density step is very large the loss of energy to internal waves is quite small; however, for small density steps the loss of energy becomes more important although the above formulation is not strictly applicable to this case as the amplitude a is then limited by the gradient and not the step.

From a practical point of view, however, it is only necessary to measure the magnitude and horizontal scale of the density fluctuations in the thermocline in order to evaluate A. Furthermore, the observed rate of deepening (as measured in § 3) of a mixed layer into a constant stable density gradient is adequately described by assuming that a constant fraction of the kinetic energy available at the interface is used to increase the potential energy of the water column. This also provides simplification for two reasons. First, it implies that, whether the turbulence is generated in the vicinity of the thermocline (for example by shear instability) or propagates from a distant source, if its local energy can be estimated then the rate of deepening can be predicted by (8). A note of caution must be added here in view of the remarks made at the end of § 3 concerning the interpretation of this agreement in terms of a relationship between the non-dimensional entrainment rate E and an interfacial Richardson number. It seems very likely that a single relationship will not exist and in fact dimensional analysis indicates that $E = E(Ri_I, Ri_G)$. A description of this functional relationship is not, however, provided by these experiments.

Second, there is a possibility that the loss of energy due to the internal waves may also be proportional to the local kinetic energy. In the early stages of the experiments described in § 3, the loss of energy to internal waves was certainly significant, and the data reflect this fact in that the deepening rate is slightly less than that given by (8). However, as the experiment progressed, even though A decreased to a value $\sim 0{\cdot}1$ there would have, in all cases, been some loss of energy to the internal waves. The fact that the data are all satisfactorily described by (8) implies that this energy loss must be absorbed by the constant c_2, indicating that the energy loss to waves is proportional to the kinetic energy input. A further indication that the energy loss is proportional to the kinetic energy input comes from the fact that the value of A after the initial stages remains approximately constant as the layer deepens, although it must be noted that it was not possible to estimate the value of A very accurately.

An indication of the importance of internal wave generation in the oceanic mixed-layer energetics is given by the following analysis of oceanic data reported by Denman & Miyake (1973). They measured mixed-layer depths at Ocean Station Papa (50° N, 145° W) in the north-east Pacific Ocean in the summer of 1970. We shall be concerned with a deepening of the mixed layer recorded during a storm from 1200 GMT 21 June to 1200 GMT 23 June 1970. During this time the mixed layer deepened from approximately 10 to 45 m, destroying an interface with a temperature difference of 0·7 °C across it as it did so. We now calculate the value of the loss parameter A for this case. Denman & Miyaki report uncertainties in the mixed-layer depth of the order of 5 m and this is used as a typical wave amplitude. This value is probably an overestimate as no account is taken of internal waves propagating along the interface, having been generated elsewhere. We shall assume that the wavelength λ is of the order of the depth (~ 20 m). Then, taking N from their profiles we find that $A \approx 5$. This large value of A indicates that even if the values of a, λ and N are overestimates a significant amount of energy would be lost to internal waves in this situation. Consequently, this implies that not only must the internal waves be included in the energetics of the oceanic mixed layer but also this deepening process may provide a significant source of internal waves in the deep ocean.

The details of the internal wave generation by the turbulent motions in the mixed layer have not been resolved by the present experiments. There appears to be a correlation between the distribution (in frequency) of energy in the interface itself and that which is manifested by the internal waves. This is entirely reasonable as we should expect the stable layer to react passively to the forcing imposed upon it. Further, the decay of the waves with vertical distance from the interface is consistent with the calculations made by Townsend (1966). Unfortunately, though, we are not in a position to trace the forcing back to the turbulence directly. To do this satisfactorily it would be necessary to know the spectral distribution of the energy in the mixed layer and this information is not available for the present experiments.

This work was supported by a grant from the Natural Environment Research Council.

Appendix. The dimensionless density profile

Following Kitaigorodskii & Miropol'skii (1970) we define dimensionless density and depth co-ordinates

$$T = [\rho_u - \rho(z,t)]/[\rho_u - \rho_h], \quad \zeta = [z - D(t)]/[h - D(t)],$$

where $D(t)$ is the depth of the upper mixed layer, of density ρ_u, and h is a reference depth at which the density remains constant at ρ_h. It is then assumed that $T \equiv T(\zeta)$, where $\zeta < 0$ refers to the mixed layer and $0 \leqslant \zeta \leqslant 1$ to the stratification through the thermocline to the reference depth h. We seek an approximate representation of $T(\zeta)$ in the form

$$T(\zeta) = \sum_{i=0}^{4} a_i \zeta^i,$$

where $T(\zeta)$ satisfies the following boundary conditions:

$$T(0) = 0, \quad T(1) = 1, \quad T'''(0) = T''(1) = 0.$$

The first two boundary conditions follow from the definitions of T and ζ. The third boundary condition comes from the requirement that the profile has maximum curvature at the bottom of the mixed layer, and the last condition from the requirement that the density gradient be constant at the reference depth h. Then

$$T(\zeta) = \zeta + a_4(5\zeta - 6\zeta^2 + \zeta^4),$$

where a_4 is determined by the value of $T'(\zeta)$ at $\zeta = 1$. Kitaigorodskii & Miropol'skii (1970) take $T'(1) = 0$ but this is inappropriate for our experiments. Evaluating $T'(\zeta)$ from our profiles we see that $T'(1) = \frac{1}{5}$, which implies that

$$T(\zeta) = 2\zeta - \tfrac{6}{5}\zeta^2 + \tfrac{1}{5}\zeta^4.$$

REFERENCES

Bouvard, M. & Dumas, H. 1967 Measurements of turbulence in water by the hot wire method. *Houille Blanche*, **22**, 257–270.

Carson, D. J. 1973 The development of a dry inversion-capped convectively unstable boundary layer. *Quart. J. Roy. Met. Soc.* **99**, 450–467.

Crapper, P. F. & Linden, P. F. 1974 The structure of turbulent density interfaces. *J. Fluid Mech.* **65**, 45–64.

Denman, L. K. & Miyake, M. 1973 Upper layer modification at Ocean Station Papa: observations and simulation. *J. Phys. Oceanog.* **3**, 185–196.

Kato, H. & Phillips, O. M. 1969 On the penetration of a turbulent layer into stratified fluid. *J. Fluid Mech.* **37**, 643–655.

Kitaigorodskii, S. A. & Miropol'skii, Yu. Z. 1970 Theory of the upper quasihomogeneous layer and seasonal thermocline in the open ocean. *Izv. Atmos. Ocean. Phys.* **6**, 97–102.

Linden, P. F. 1973 The interaction of a vortex ring with a sharp density interface: a model for turbulent entrainment. *J. Fluid Mech.* **60**, 467–480.

Niiler, P. P. 1975 Deepening of the wind-mixed layer. Submitted to *J. Mar. Res.*

Thompson, S. M. & Turner, J. S. 1975 Mixing across an interface due to turbulence generated by an oscillating grid. *J. Fluid Mech.* **67**, 349–368.

THORPE, S. M. 1966 Internal gravity waves. Ph.D. thesis, University of Cambridge.

THORPE, S. M. 1973 Turbulence in stably stratified fluids: a review of laboratory experiments. *Boundary-Layer Met.* **5**, 95–119.

TOWNSEND, A. A. 1966 Internal waves produced by a convective layer. *J. Fluid Mech.* **24**, 307–319.

TURNER, J. S. 1968 The influence of molecular diffusivity on turbulent entrainment across a density interface. *J. Fluid Mech.* **33**, 639–656.